DOI: 10.1126/science.232.4746.54

Reports

The Geochemical Behavior of Aluminum in Acidified Surface Waters

Darrell Kirk Nordstrom and James W. Ball

Speciation calculations for aluminum, in water samples taken from a drainage basin containing acid mine waters, demonstrate a distinct transition from conservative behavior for *p*H below 4.6 to nonconservative behavior for *p*H above 4.9. This transition corresponds to the *pK* for the first hydrolysis constant of the aqueous aluminum ion and appears to be a consistent phenomenon independent of field location, ionic strength, and sulfate concentration. Nonconservative behavior is closely correlated with the equilibrium solubility of a microcrystalline gibbsite or amorphous aluminum hydroxide.

Although considerable research effort has been expended on studying the chemistry of aluminum in surface waters affected by acid rain, progress has been slow and difficult because of (i) the complexity of reactions involving aluminum, (ii) the difficulty of sampling, preservation, and analysis, (iii) the discrepancies in thermodynamic data used for computations of chemical equilibrium, (iv) the lack of useful kinetic data, and (v) the dynamic state of natural open systems. Driscoll has demonstrated a method for separating organically bound dissolved aluminum from inorganic dissolved aluminum (*1*); his results show a strong correlation between total organic carbon and organically bound aluminum for surface waters in the Adirondacks (*2*). Furthermore, speciation calculations that use the concentration of the separated inorganic aluminum exhibit saturation with respect to microcrystalline and natural gibbsite, $Al(OH)_3$ (*2, 3*). Pertinent thermodynamic data on solubility product constants for various forms of gibbsite, the first two hydrolysis constants, and the fluoride and sulfate ion-pair stability constants are well established (*4, 5*). These studies have made the geochemistry of aluminum in acid aquatic systems much more amenable to quantitative interpretation.

A further complication arises from the suggestion that basic aluminum sulfate minerals may control aluminum concentrations in waters having low *p*H and high sulfate concentrations (*6–8*). Nordstrom (*8*) pointed out that for *p*H values less than about 4.5 natural waters frequently appear undersaturated with respect to gibbsite and kaolinite, and their aluminum concentrations might be related to the solubilities of such minerals as alunite, $KAl_3(SO_4)_2(OH)_6$, jurbanite, $Al(SO_4)OH \cdot 5H_2O$, and basaluminite, $Al_4(SO_4)(OH)_{10} \cdot 5H_2O$.

The purpose of examining the saturation condition of natural waters with respect to any relevant minerals via equilibrium calculations is to provide a reference state. Many systems will be in a state of disequilibrium, but such a disequilibrium state cannot be determined without knowledge of the equilibrium state, together with a proper understanding of the hydrogeologic conditions, an appraisal of sources of error, and proper methods of data presentation. It is the purpose of this report to demonstrate that, when a broad enough range of *p*H has been measured, aluminum shows both conservative (nonreacting) and nonconservative (reacting) behavior in acidified stream waters, with a transition from one to the other in the *p*H range 4.5 to 5.0. This dual behavior helps to explain patterns in aluminum concentrations for natural waters as a function of *p*H.

During 1981–82 we took more than 60 water samples from a drainage basin receiving acid mine waters from the Leviathan mine in Alpine County, California. The acid effluent enters near the headwaters of Leviathan Creek and is diluted by downstream tributaries. Metal concentrations are attenuated by dilution, adsorption, and precipitation during downstream transport through the Leviathan Creek–Bryant Creek–Carson River system. Samples were filtered on site through 0.1-μm pore-size membranes in acid-cleaned plastic filters into previously cleaned high-density polyethylene containers with portable peristaltic pumps. Ultrapure nitric acid was used to acidify the samples to *p*H <1.5 for major and trace cation determinations. Unacidified samples were used for anion determinations. Aluminum was determined by direct-current, argon-plasma emission spectroscopy.

Values of *p*H ranged from 1.8 to 8.8, and aluminum concentrations ranged from <0.01 to 620 mg/liter (*9*). Complete analyses for 40 major and trace constituents were obtained (*9*), and free-ion and ion-pair activities were computed from these results by means of the WATEQ3 computer program (*10*). Values of the activity *a* of aqueous Al^{3+} are plotted as a function of *p*H in Fig. 1. The error in the field *p*H measurement is ±0.05, and the error in *a* is 5 to 25 percent, depending on the concentration range and the *p*H. Hence, the error in each data point is no larger than the area covered by the plot symbol. A striking pattern emerges in which there are essentially two near-linear slopes that intersect in the *p*H range 4.5 to 5.0. The steeper slope (plus symbols in Fig. 1) corresponds to the solubility of a fine-grained or microcrystalline gibbsite to amorphous $Al(OH)_3$ on the basis of reliable solubility data (*4, 5*). The best linear fit gives a slope of −3.11 (standard error = 0.21). This stoichiometric match with gibbsite solubility is strikingly consistent with the field data of Driscoll and co-workers (*2, 3*) for Adirondack surface waters affected by acid rain; this match is also consistent with the laboratory data of May *et al.* (*4*), which demonstrate that equilibrium solubility for gibbsite can be reached within 2 hours for neutral *p*H conditions from over- or undersaturation.

The shallower slope (open squares in Fig. 1) was puzzling because a possible solubility control by basic aluminum sulfate minerals was anticipated, yet the Al:OH molar ratio for this slope is 1.7, which does not correlate with any known aluminous mineral. However, a comparison of the total filterable aluminum concentrations with the sulfate concentrations (Fig. 2) shows a positive linear slope of 1.21 (standard error = 0.022) for *p*H <4.6 (open squares), implying conservative behavior. Sulfate is a good nonreactive tracer for mine waters because it is usually present in very high concentrations in the acid effluent (up to 11,000 mg/liter at Leviathan) but very low concentrations in normal stream waters (a few milligrams per liter), and it is strongly correlated with injected chloride from tracer studies (*11*). Chemical processes that might remove sulfate are negligible by comparison to dilution processes, within the errors of the measurements. The excellent fit of the slope of aluminum plotted against sulfate at low *p*H not only indicates conservative behavior but it is also derived from the same set of values that occur for *p*H <4.6 in Fig. 1. The shallow slope shown in Fig. 1 is a mixing line reflecting dilution of the original acid mine effluent, and it has little chemical sig-

---

U.S. Geological Survey, 345 Middlefield Road, Menlo Park, CA 94025.

nificance. Above a pH of about 4.6, further neutralization leads to the formation of microcrystalline gibbsite or amorphous $Al(OH)_3$ that controls $a_{Al^{3+}}$. The transition from pH 4.6 to pH 4.9 is close to the first hydrolysis constant for Al^{3+} at a pK of about 5.0 (*5, 12, 13*), and the beginning of hydrolysis helps to initiate the onset of gibbsite precipitation. The beginning of hydrolysis of the aqueous Al^{3+} (or rather deprotonation of the six-coordinated hydration sphere of aluminum) makes possible olation, the bridging of bonds between the oxygens of different hydrated aluminum ions, so that crystal growth can occur (*13*). Dilution of the sulfate at higher pH values helps to decrease sulfate complexing and also to increase deprotonation (*13, 14*); consequently, polymerization and precipitation occur much more rapidly at pH values above 4.6 (*15*). This mechanism also explains the excellent correlation between the first hydrolysis constants and the solubility product constants for metal hydroxides (*16*).

The aluminum-pH transition zone is substantiated in other reports of similar data: figure 7 of Driscoll *et al.* (*2*), figure 1 of Hooper and Shoemaker (*17*), and figure 12 of Crouse and Rose (*18*). The two lines that represent the best fit of our data are shown in Fig. 3; data points from Driscoll *et al.* (*2*) and Crouse and Rose (*18*) are also shown. The data of Hooper and Shoemaker (*17*) are too numerous to plot, but they directly overlie the data of Driscoll *et al.* (*2*). Although differences exist in the intercepts, a break in slope at $pH = 4.5$ to 5.0 is demonstrated. The consistency between these data, which have been taken from different field sites and which have different ionic strengths and sulfate concentrations, attests to the universality of this phenomenon. The correspondence of the transition zone to the first hydrolysis constant for aqueous Al^{3+} provides a basis for the phenomenon and its universal nature.

Two important questions remain unresolved. What might control the initially high concentrations of aluminum in the most acid mine effluent? How might aluminum behave at $pH < 4.6$ in soil or ground-water systems, for example, those affected by acid rain?

Two possible controls on the aluminum chemistry of acid mine effluent are (i) the leaching rate of aluminum from common aluminosilicate minerals in sulfuric acid solutions and (ii) the solubility of basic aluminum sulfate minerals known to exist under these conditions. Unfortunately, acid errors for glass pH electrodes can be rather large at these low pH values (*19*), and chemical equilibrium computations have large uncertainties due to unknown or unreliable data on stability constants and activity coefficients. More research on electrolyte thermodynamics and acid pH errors and additional field data are needed to resolve this question.

Subsurface waters have greatly increased residence times, and they will be exposed to much larger surface areas of minerals per unit time than surface waters. Hence, they should exhibit increasing tendencies toward mineral saturation with basic aluminum sul-

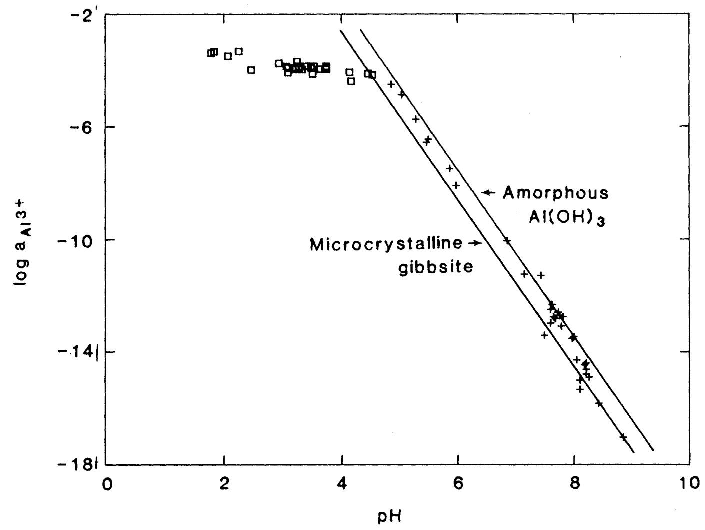

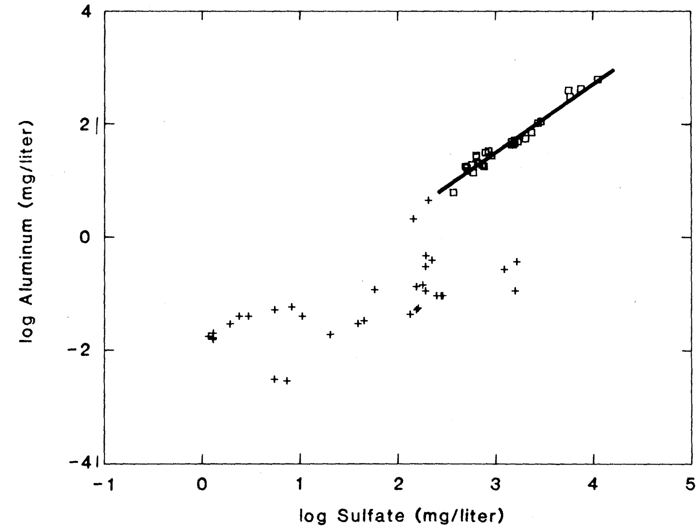

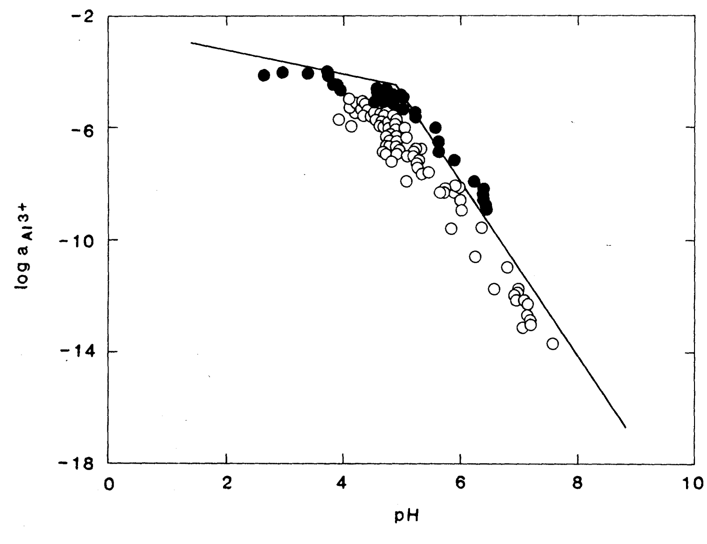

Fig. 1 (upper left). Plot of log $a_{Al^{3+}}$ versus pH for 64 samples from a drainage basin containing acid mine waters from the Leviathan mine, California-Nevada. Data points shown by open squares represent those with $pH < 4.6$, plus symbols those with $pH > 4.9$. The two solid lines show the solubilities for amorphous $Al(OH)_3$ and microcrystalline gibbsite (*5*). Fig. 2 (upper right). Plot of aluminum concentrations versus sulfate concentrations for the same samples as in Fig. 1 and with the same symbols. Fig. 3 (lower left). Plot of log $a_{Al^{3+}}$ versus pH for acid mine drainage from Appalachia (*18*, represented by closed circles) and Adirondack lake waters affected by acid precipitation (*2*, represented by open circles).

fate phases at low *p*H. The data of Driscoll *et al.* (*2*) are from Adirondack lakes, which should have greater mineral contact time than Leviathan stream waters. This greater residence time could be reflected in the bias of their data toward lower free aluminum *a* values, representing the solubility of a more stable phase of gibbsite (Fig. 3). In addition, the aluminum concentrations in Adirondack lake waters were achieved from undersaturation by dissolution of aluminosilicates by acidified meteoric input, whereas those in the Leviathan drainage waters were achieved from supersaturation by dilution. Hence, a range of gibbsite stoichiometries might be achieved in natural waters that reflect the residence time of the water. For *p*H <4.6 the Leviathan data should reflect the maximum aluminum activities derived by simple mixing, whereas lower activities, down to the limits of alunite or jurbanite solubilities, should reflect increased residence times.

REFERENCES AND NOTES

1. C. T. Driscoll, *Int. J. Environ. Anal. Chem.* **16**, 267 (1984).
2. ———, J. P. Baker, J. J. Bisogni, C. L. Schofield, in *Geological Aspects of Acid Precipitation*, O. P. Bricker, Ed. (Butterworth, London, 1984), p. 55.
3. N. M. Johnson, C. T. Driscoll, J. S. Eaton, G. E. Likens, W. H. McDowell, *Geochim. Cosmochim. Acta* **45**, 1421 (1981).
4. H. M. May, P. A. Helmke, M. L. Jackson, *ibid.* **43**, 681 (1979).
5. D. K. Nordstrom, S. D. Valentine, J. W. Ball, L. N. Plummer, B. F. Jones, *U.S. Geol. Surv. Water-Resour. Invest. Rep. 84-4186* (1984).
6. N. van Breemen, *Soil Sci. Soc. Am. Proc.* **37**, 694 (1973).
7. E. Eriksson, *Nord. Hydrol.* **12**, 43 (1981).
8. D. K. Nordstrom, *Geochim. Cosmochim. Acta* **46**, 681 (1982).
9. J. W. Ball and D. K. Nordstrom, *U.S. Geol. Surv. Water-Resour. Invest. Rep. 85-4169* (1985).
10. J. W. Ball, E. A. Jenne, M. W. Cantrell, *U.S. Geol. Surv. Open-File Rep. 81-1183* (1981).
11. K. Bencala, D. M. McKnight, G. W. Zellweger, in preparation.
12. C. F. Baes, Jr., and R. E. Mesmer, *The Hydrolysis of Cations* (Wiley-Interscience, New York, 1976).
13. J. D. Hem and C. E. Roberson, *U.S. Geol. Surv. Water-Supply Pap. 1827-A* (1967).
14. J. D. Hem, *U.S. Geol. Surv. Water-Supply Pap. 1827-B* (1968).
15. R. W. Smith and J. D. Hem, *U.S. Geol. Surv. Water-Supply Pap. 1827-D* (1972).
16. W. Stumm and J. J. Morgan, *Aquatic Chemistry* (Wiley-Interscience, New York, 1981).
17. R. P. Hooper and C. A. Shoemaker, *Science* **229**, 463 (1985).
18. H. L. Crouse and A. Rose, "Natural benefication of acid mind drainage by interaction of stream sediment," *Sixth Symposium on Coal Mine Drainage Research* (National Coal Association/Bituminous Coal Research, Louisville, KY, 1976), p. 237.
19. S. L. Stipp, thesis, University of Waterloo (1983).

20. We acknowledge the helpful review comments provided by J. D. Hem, B. F. Jones, H. M. May, and G. A. Parks.

21 October 1985; accepted 6 February 1986

Interannual Variability of Atmospheric Methane: Possible Effects of the El Niño–Southern Oscillation

M. A. K. KHALIL AND R. A. RASMUSSEN

Nearly continuous measurements at Cape Meares, Oregon, revealed that methane was increasing in the earth's atmosphere and that its concentration varied cyclically with the seasons. After 6 years of measurements, results show that the rate of increase in methane undergoes interannual variations; the most prominent of these coincided with the last major El Niño–Southern Oscillation, when methane concentrations fell far below expected levels. One of the consequences of the interannual variability is that the long-term rate of increase at Cape Meares is now about 16 parts per billion by volume per year, or about 1 percent annually, which is significantly less than that indicated by the earliest calculations.

UNTIL A FEW YEARS AGO, IT WAS believed that the concentration of methane (CH_4) in the atmosphere is unchanging. Recent experiments have shown, however, that it not only varies with latitude and the seasons, but is steadily increasing in the earth's atmosphere (*1, 2*). Here we report that the rate of increase is not constant and that El Niño–Southern Oscillation (ENSO) (*3*) events may trigger substantial short-term variations in atmospheric CH_4.

Table 1. Effects of interannual variability of CH_4 and the long-term rate of increase at Cape Meares. The annual rates of increase in parts per billion by volume and percent are based on the models $C = a + bt$ and $C = a\exp(bt)$, respectively, where C is the monthly average concentration. The initial value reflects the calculated concentration in the first month of each period. N is the number of data and months in each period. The ±values are the 90 percent confidence limits for the rate of increase over the times spanned by each segment of the data (t-statistic) (*12*). $S_{yx} = [\Sigma_i d_i^2/N - 2]^{1/2}$, where $d_i = (C_i - \hat{C}_i)$ are the deviations of the measured concentrations (C_i) from those predicted by the model equations ($\hat{C}_i$).

Item	Jan. 1979 to Aug. 1980	Aug. 1981 to May 1982	May 1982 to Feb. 1983	Feb. 1983 to Jan. 1985	Average (total)
Annual rate of increase ($b + \delta b$)					
ppbv	29 ± 6	14 ± 3	−3	13 ± 3	16
Percent	1.8 ± 0.3	0.8 ± 0.2	−0.2	0.8 ± 0.2	1.0
a (ppbv)	1603	1652	1676	1673	1661 ± 5*
N	20	21	9	22	72
S_{yx} (ppbv)	7	7	9	5	5

*Mean of all the data.

The increase in CH_4 is probably attributable to industrial and agricultural activities. Over the past century, human activities may also have depleted the concentration of hydroxyl (OH) radicals in the troposphere, thus reducing the capacity of the atmosphere for removing CH_4 and many other trace gases (*4*). The concentrations of CH_4 found in bubbles of air extracted from polar ice cores suggest that these processes of increasing emission and of decreasing removal have caused atmospheric CH_4 to more than double over the past 200 years (*4, 5*). A continued increase in CH_4 could cause global climatic changes, including warming of the earth by adding to the greenhouse effect and changes in the physics and chemistry of the earth's atmosphere (*6*).

For more than 6 years we have made continuous measurements of CH_4 at Cape Meares on the Oregon coast (45°N, 124°W) using an automated gas chromatographic system with a flame ionization detector (*1, 7*). Early results suggested that atmospheric CH_4 is increasing and provided an estimate of the rate of increase (*1*). Measurements at other locations from the arctic to the South Pole have confirmed that the trends observed at Cape Meares are representative of a global change. Now the record is sufficiently complete to allow the interannual variability of the trends to be evaluated.

The rate of increase does indeed vary from year to year. The largest of the short-term variations coincided with the last (and somewhat anomalous) ENSO event of 1982 to

---

Institute of Atmospheric Sciences, Department of Chemical, Biological, and Environmental Sciences, Oregon Graduate Center, Beaverton, OR 97006.